Thermal Chemistry of Tetrakis(ethylmethylamido)titanium on Si(100) Surfaces†

Byung-Chang Kan, Jin-Hyo Boo,‡ Ilkeun Lee, and Francisco Zaera*

Department of Chemistry, University of California, Riverside, California 92521

Received: November 20, 2008; Revised Manuscript Received: February 17, 2009

The thermal chemistry of tetrakis(ethylmethylamido)titanium (TEMAT) on (100)-oriented surfaces of silicon wafers was studied by using infrared absorption and X-ray photoelectron spectroscopies. Dissociative adsorption was identified starting at temperatures around 450 K, likely limited by the rate of an initial elimination of some of the amido groups. That adsorption is rapidly followed by a selective β-hydride elimination reaction from the ethyl moiety of the remaining ligands to produce *N*-methylethylidenimine adsorbed species. Long exposures of the Si(100) surface to TEMAT above the temperature of decomposition lead to the growth of a metal nitride film. Those films appear to grow in 3-D fashion, and contain high levels of C and O contaminants.

1. Introduction

Below we report results from our studies on the thermal chemistry of tetrakis(ethylmethylamido)metal complexes (TEMAM, metal = Ti, Zr, Hf) on Si(100) surfaces, focusing in particular on the titanium compound (TEMAT). These and similar metal amido complexes have been tested over the years for the growth of metal nitride[1,2] and metal oxide[3,4] films by both standard chemical vapor deposition (CVD)[5−7] and, more recently, atomic layer deposition (ALD) methods.[8−10] Metal amido complexes are often volatile, can be made to react at relatively low temperatures, produce noncorrosive byproducts, and often leave fewer impurities in the growing films.[7,11] On the other hand, they are thermally unstable, and may display undesirable side chemistry.[12−14] The optimization of the use of metal amido complexes for film deposition can benefit greatly from a better molecular-level understanding of their thermal and surface chemistry.

Several studies have already been published on some aspects of the surface chemistry of the most common metal amido compounds, in particular tetrakis(dimethylamido) (TDMAM),[1,2,15−20] tetrakis(diethylamido) (TDEAM),[2,16,21−23] and tetrakis(ethylmethylamido) (TEMAM) complexes.[2,14,24−27] Most of the work cited above has focused on the use of these compounds as precursors in ALD processes, but additional reports are also available on some molecular aspects of the surface chemistry of those compounds.[15,28−35] Nevertheless, most of the questions associated with the mechanism of reaction of these compounds on surfaces remain unanswered. For instance, it is often assumed that the adsorption of these compounds may be dissociative, accompanied by the loss of some of the amido ligands. However, although this is a reasonable assumption if an increase in metal coordination number and a possible oxidation of the metal center is to be avoided, proof for this step is still lacking; it is not even clear in what form the amido ligands may be eliminated.[36]

There is also very limited knowledge of what happen to the remaining ligands upon thermal activation. A number of surface reactions have already been identified in the past, including oligomerizations[28,29] and β-hydride eliminations:[29] the former can take place in the gas phase and may very well be responsible for the initiation of the deposition of solid films, and the latter has received quite a bit of attention in studies related to CVD and ALD with amido complexes,[37] perhaps because it may help account for the deposition of carbon and nitrogen impurities during the growth of metal nitride layers. Convincing evidence for β-hydride elimination has in fact been obtained by detailed surface-science experiments.[30] One suggestion advanced by some authors is that the β-hydride elimination step may be accompanied by reductive elimination of another amido ligand with the hydrogen released (to produce an amine), in what amounts to a disproportionation reaction.[37] A more complicated proposal is that of an intermolecular dehydrogenation surface step to form metal−N−C−metal bridges.[32] Regardless, dehydrogenation steps such as these do involve redox chemistry, and could account for the reduction of the metal on their way to form metal nitrides. As with the metal halides,[38−40] the metal amido complexes could act as their own reducing agent.

In this paper, results from our studies on the fundamental chemistry of TEMAM on Si(100) surfaces aimed at addressing some of the mechanistic questions posed above are reported. Infrared absorption and X-ray photoelectron spectroscopy data point to a dissociative and activated adsorption leading to partly decomposed metal-containing adsorbed species. The rate-limiting step for the adsorption was inferred to be the displacement of some of the amido ligands. The activated nature of the TEMAM adsorption sets a lower limit on the temperature needed for the growth of metal nitride or metal oxide films, at approximately 475 K for the case of TEMAT. Dissociative adsorption is followed immediately by a β-hydride elimination step from the ethyl moiety of the remaining coordinated amido groups to produce a surface *N*-methylethylidenimine species, and to the growth of three-dimensional nitride films with high levels of C and O contaminants.

2. Experimental Section

The infrared (IR) absorption spectroscopy data reported below were obtained in one of two instruments specifically designed for surface characterization experiments in ALD processes. The first instrument, shown schematically in Figure 1, was built around a 2¾ in. outside diameter, 0.75 in. thick, double-sided

† Part of the "George C. Schatz Festschrift".

* Corresponding author. E-mail: zaera@ucr.edu.

‡ Permanent Address: Department of Chemistry, Sungkyunkwan University, Suwon 440-746, Korea.

10.1021/jp8102172 CCC: $40.75
Published on Web 03/10/2009

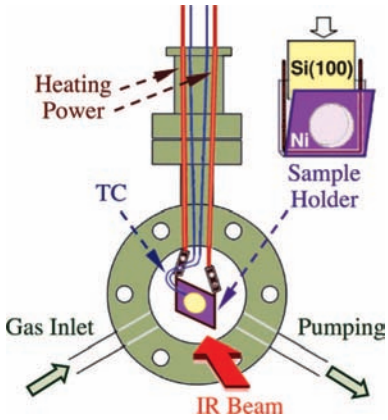

Figure 1. Schematic representation of the cell used for in situ transmission infrared absorption spectroscopy surface characterization experiments. The system was built around a 2¾ in. double-sided Conflat flange, the cross section of which is shown in green, and has lines for gas dosing and pumping as well as a port for the handling and heating of the silicon substrate. A more detailed diagram of the mounting scheme for the surface is shown in the upper right corner, pointing to the nickel pocket used to hold and resistively heat the Si(100) wafer. The IR beam travels in the direction perpendicular to the plane of the page and goes through the front and back NaCl windows used to cap this reactor. The surface is placed at a ~45° angle from the beam.

ultrahigh vacuum (UHV) Conflat flange capped on both sides (front and back) with NaCl windows. The enclosed volume could be filled to pressures of up to approximately 1 atm of the desired gases, exposed to a continuous flow of those gases at atmospheric pressure, or pumped to a vacuum in the mTorr range by using the two 1/4 in. stainless-steel access tubes located on the sides of the bottom half of the main flange. A mini (1.33" diameter) Conflat flange port was added on the top for sample insertion. The sample, an approximately 1 cm × 1 cm square Si(100) wafer polished on one side, was mechanically mounted inside a tight pocket made out of a 0.1 mm thick nickel foil that also operates as a resistive heater. A 6 mm diameter hole was placed in the middle of the nickel pocket to expose the silicon sample to the gases and to allow for the passage of the infrared beam. The complete assembly was held via nickel wires spotwelded to the sides of the Ni pocket and attached via copper barrel connectors to the electrical feedtroughs of the mini-flange used as manipulator. With this arrangement, the sample could be heated to temperatures up to approximately 650 K, as measured by a chromel−alumel thermocouple attached to the side of the silicon wafer, and set using a proportional-integral-derivative (PID) controller and a variable transformer. This cell was placed at the focal point of the infrared beam of the sample compartment of the Fourier-transform infrared absorption spectrometer for data acquisition in transmission mode, with the sample mounted at an angle of approximately 45° with respect to the direction of the beam. Our setup shares some similarities with that described by Chabal and co-workers.[34] Blank experiments where the sample was replaced by a KBr window were carried out to evaluate any potential interference from adsorption on the optical elements of the cell, a problem that could be minimized and that did not affect the results reported here. By removing the solid substrate from the manipulator, the cell described here could also be used to acquire the infrared spectra of the TEMAM precursors in the gas phase.

A second setup was built to perform IR absorption spectroscopy experiments in an attenuated total reflection (ATR) mode (Figure 2). In this case the reactor volume was made out of a 2¾ in. outside diameter, 0.75 in. thick, double-sided ultrahigh

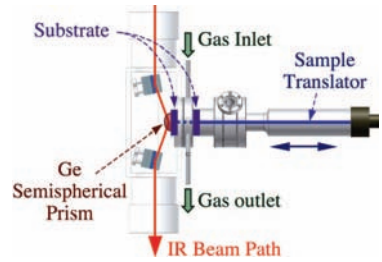

Figure 2. Schematic representation of the cell designed for attenuated total reflection (ATR) infrared absorption spectroscopy surface characterization experiments. In this case the silicon wafer is placed at the end of a linear device used to transfer the surface back and forth between the center of the reactor and the germanium semispherical prism used as the optical element for ATR.

vacuum (UHV) Conflat flange coupled to a 1.75 in. long stainless-steel nipple terminated in 2¾ in. Conflat flanges. A mini-flange port was added to the side of the double-sided flange for the attachment of the electrical feedtroughs, as before, but the gas inlet and outlet lines were placed on the far-end flange of the nipple. That flange was terminated with another 2¾ in. Conflat flange, custom modified to hold a 1.25 cm diameter germanium semispherical prism used as the window for the passage of the infrared beam. A linear translation manipulator was bolted to the opposite side of the double-sided flange. A similar 1 cm × 1 cm square Si(100) wafer to that used in the transmission IR experiments was mounted at the end of this manipulator by gluing it with a silver paste to a homemade heater consisting of a U-shaped, 0.1 mm thick, nickel foil wrapped around a T-shaped ceramic holder attached to the end of the translation rod that served as both insulator for the heater and supporter of it and its electrical connectors. In this arrangement the Ni foil could be heated resistively to temperatures of up to ~675 K by using AC current fed via copper feedtroughs attached to a side flange of the reactor, and the temperature measured by a chromel−alumel thermocouple spotwelded to the nickel foil and set using a PID controller and a variable transformer. Stable temperatures could be reached within 2 min, and held constant to approximately ±2 K.

In the ATR cell, the sample was pressed against the Ge prism to acquire the IR spectra, and retracted to place it inside the volume of the reactor for gas exposure. In our arrangement the beam is focused on only one point on the sample, and collected after a single reflection. A spatially resolved study of the performance of our ATR instrument indicated that most of the signal originates from the central ~3 mm diameter area of the sample. All spectra in the experiments with both transmission and ATR setups were collected by using a Bruker Tensor 27 Fourier-transform infrared spectrometer (FTIR). Most of the data were acquired by using a liquid nitrogen-cooled mercury−cadmium−telluride (MCT) detector, but some were taken by employing a deuterated−triglycerine−sulfate (DTGS) detector instead. The spectra reported here correspond to the addition of 1024 scans taken at a resolution of 4 cm^{-1}, a process that takes approximately 7−8 min. All spectra obtained for the surfaces after gas dosing were referenced to similar data acquired right before any gas exposures.

In all our studies, square 1 cm × 1 cm Si(100) wafers (Silicon Valley Microelectronics) were used as the substrate. The front surface was polished and washed with acetone before introduction into the IR cells, but no further treatment was followed. In particular, no etching treatments were performed, so the surface retained the thin silicon oxide layer that grows naturally on silicon wafers.[41] The TEMAM precursors were dosed via direct

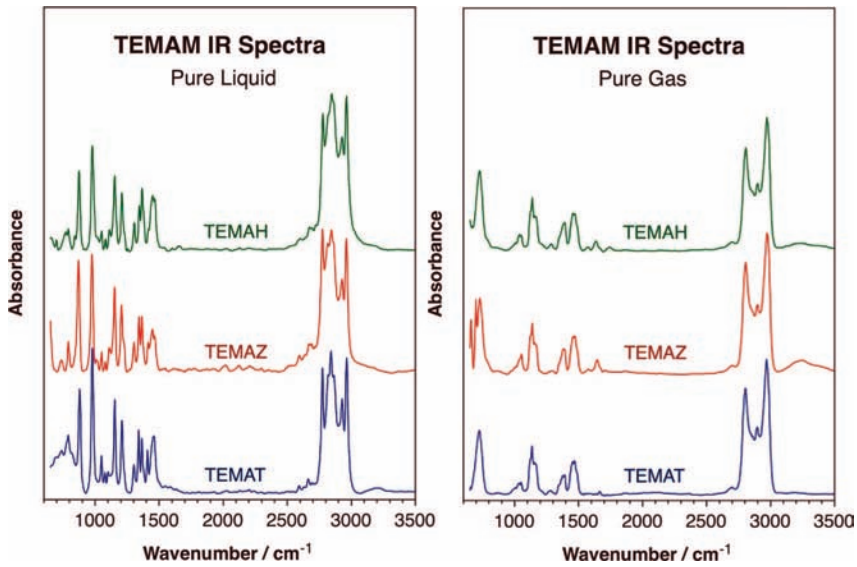

Figure 3. Infrared absorption spectra of TEMAT, TEMAZ, and TEMAH in both liquid (left panel) and gas (right panel) phases. The spectra of all three compounds are quite similar, indicating that they are dominated by the vibrational modes of the amido ligands. On the other hand, significant differences are seen between the data for the liquid and gas phases because of the different rate of interconversion among the various possible rotational conformers of these compounds.

evaporation of the liquids, by gently heating both the container and the gas-handling manifold, to 340 and 355 K, respectively; their pressure in the IR cells was controlled via throttling of the input line. The dosing experiments were carried out in one of two modes designed to minimize exposure of the surface to contaminants: (1) by statically filling the reactor volume with the gases of interest for a specified amount of time and pumping afterward or (2) by continuously flowing the gases through the cell during dosing with the aid of an inert carrier gas (typically nitrogen). In all cases, the volume of the cell was thoroughly pumped in between exposures, and in most cases also purged with an inert gas, either argon or nitrogen. All TEMAM (M = Ti, Zr, or Hf, all from Sigma Aldrich, ≥99% purity, 99.99+% metal purity) and all gases (Ar: Airgas, 99.998% purity; N_2: Airgas, 99.998% purity) were used as supplied.

Ex situ X-ray photoelectron spectroscopy (XPS) characterization of the grown films was carried out by using a Leybold EA11-MCD system equipped with a dual Mg Kα (1253.6 eV)/Al Kα (1486.6 eV) X-ray source, a 100-mm electron energy concentric hemispherical analyzer, and a 18-channel multichannel detector.[38,42] Survey spectra (scans of 1000 eV or more in width) were taken by using a band-pass energy of 100 eV, which corresponds to a spectral resolution of approximately 2.0 eV, and additional narrow scans of the main photoelectron lines were obtained with a band-pass energy of 31.5 eV (which yields a total resolution of ~0.9 eV). To compensate for any charging effects, all of the XPS peak positions were referred to the Si 2p peak at 99.15 eV.[43]

3. Results

3.1. Infrared Characterization of TEMAM Compounds. Since our studies on the adsorption and surface chemistry of the tetrakis(ethylmethylamido) metal (TEMAM) compounds rely mainly on the use of infrared absorption spectroscopy, an assignment of the vibrational modes of those compounds was attempted first. Spectra for the three compounds, with titanium, zirconium, and hafnium, are reported in both liquid and gas phases in Figure 3. Two things become apparent upon simple inspection of this figure: (1) the spectra of all three TEMAM are quite similar, an indication that the vibrational modes observed are all associated with the amido ligands, and (2) the spectra obtained in the liquid differ significantly from those recorded in the gas phase. This latter observation is due, at least in part, to the different rate at which the compounds interconvert among their multiple rotational conformers in the two phases, as has already been documented for the amines alone.[44−47] In general, the molecules in the gas phase rotate more freely than those in the liquid phase, so the IR absorption bands represent an average over all conformers, and are therefore typically broader and less well resolved.

The assignment of the bands in Figure 3 was made with the help of a number of reports from the literature, including previous assignments made for methylamine,[47,48] ethylamine,[47,49,50] propylamine,[47,51] dimethylamine,[47,52,53] diethylamine,[53] trimethylamine,[47,54] ethylmethylamine,[45,46,53] dimethylethylamine,[44] and ethyldimethylamine-borane.[55] Comparisons were also made to the few reported assignments of IR spectra for tetrakis(dimethylamido)titanium (TDMAT),[28,32,56−59] tetrakis(dimethylamido)zirconium (TDMAZ),[60] tetrakis(diethylamido)titanium (TDEAT),[57,61] tetrakis(ethylmethylamido)titanium (TEMAT),[62] and tetrakis(ethylmethylamido)hafnium (TEMAH).[63] For the sake of this discussion, the data in Figure 3 can be divided into three sections: (1) between 700 and 1600 cm^{-1}, where most of the molecular deformation modes are seen; (2) between 1600 and 2700 cm^{-1}, a range virtually flat in these traces where vibrational modes would be seen for stretching modes of carbon−nitrogen multiple bonds and/or N−H deformations; and (3) between 2700 and 3100 cm^{-1}, the region where the C−H stretching vibrations are observed. A fourth sector above 3100 cm^{-1}, where N−H stretching modes are typically detected, is also generally silent here.

The assignment of the deformation mode region of these spectra can be somewhat difficult, because (1) most modes there are not pure but rather combinations of several concerted molecular motions and (2) many deformation vibrational frequencies are heavily dependent on the different rotational conformations possible for these molecules. The latter is the likely reason for the differences in the spectra of these compounds seen between the gas and liquid phases, as mentioned above. Nevertheless, the assignment of the infrared

TABLE 1: Vibrational Assignment (in wavenumbers) of the Peaks in the Infrared Absorption Spectra of TEMAT, TEMAZ, and TEMAH in Both Liquid and Gas Phases

	liquid[b]			gas[b]		
mode[a]	TEMAT	TEMAZ	TEMAH	TEMAT	TEMAZ	TEMAH
$\rho(CH_2)$	791 (m)	792 (m)	790 (m)	726 (s)	726 (s)	726 (s)
$\rho(CH_3)_{Et}$, $\nu(C-C)$	878 (s)	871 (s)	874 (s)	870 (vw)	870 (vw)	870 (vw)
$\rho(CH_3)_{Et}$, $\nu(C-C)$	978 (vs)	975 (vs)	978 (vs)	1001 (w)	1008 (vw)	1006 (vw)
$\nu_s(C-N-C)$	1050 (m)	1051 (m)	1051 (m)	1052 (w)	1053 (w)	1054 (w)
$\nu_{as}(C-N-C)_{trans}$				1135 (m)	1136 (m)	1137 (m)
$\nu_{as}(C-N-C)_{gauche}$	1153 (s)	1153 (s)	1154 (s)	1156 (m)	1156 (m)	1156 (m)
$\nu_{as}(C-N-C)_{gauche}$				1170 (m)	1170 (m)	1170 (m)
$\rho(CH_3)_{Me}$	1209 (s)	1206 (s)	1208 (s)	1205 (vw)		1210 (vw)
$\omega(CH_2)$	1302 (m)	1303 (m)	1305 (m)	1275 (br)	1290 (vw)	1273 (vw)
$\tau(CH_2)$	1339 (s)	1342 (s)	1343 (s)	1338 (sh)	1338 (sh)	1338 (sh)
$\delta_s(CH_3)_{Et}$	1364 (s)	1363 (s)	1367 (s)	1363 (m)	1367 (m)	1368 (m)
$\delta_s(CH_3)_{Me}$	1370 (sh)	1368 (sh)	1371 (sh)	1376 (m)	1378 (m)	1380 (m)
$\gamma(CH_2)$	1408 (m)	1412 (m)	1415 (m)	1392 (m)	1393 (m)	1393 (m)
$\delta_{as}(CH_3)_{Et}$	1438 (sh)	1435 (sh)	1436 (sh)	1442 (w)	1442 (w)	1442 (sh)
$\delta_{as}(CH_3)_{Me}$	1450 (s)	1448 (s)	1449 (s)	1452 (m)	1453 (m)	1454 (m)
$\delta_{as}(CH_3)_{Me}$	1460 (s)	1465 (s)	1467 (s)	1471 (m)	1472 (m)	1472 (m)
$\delta_{as}(CH_3)_{Et}$			1493 (vw)	1490 (w)	1492 (w)	1492 (w)
$2 \times \delta(CH_3)$	2774 (vs)	2775 (vs)	2778 (vs)			
$\nu_s(CH_3)_{Me}$	2818 (s)	2813 (s)	2815 (s)	2804 (vs)	2806 (vs)	2805 (vs)
$\nu_s(CH_2)$	2842 (vs)	2844 (vs)	2847 (vs)	2845 (sh)		2850 (sh)
$\nu_s(CH_3)_{Et}$	2862 (s)	2862 (s)	2863 (s)	2860 (m)	2862 (m)	2863 (m)
$\nu_s(CH_3)_{Et}$				2898 (s)	2899 (s)	2900 (s)
$\nu_{as}(CH_2)$	2927 (m)	2928 (m)	2927 (m)			
$\nu_{as}(CH_3)_{Me,Et}$	2963 (vs)	2962 (vs)	2962 (vs)	2968 (vs)	2971 (vs)	2971 (vs)
$\nu_{as}(CH_3)_{Me}$				2977 (vs)	2979 (vs)	2979 (vs)

[a] Vibrational modes: ρ = rocking, ν = stretching, ω = wagging, τ = twisting, δ = deformation, γ = scissoring. Subindices: s = symmetric, as = asymmetric, Me = methyl moiety, Et = ethyl moiety. The subindices "trans" and "gauche" refer to rotational conformers of the amido ligands. [b] Signal intensities: vs = very strong, s = strong, m = medium, w = weak, vw = very weak, br = broad, sh = shoulder.

absorption features between 1350 and 1600 cm^{-1} is fairly straightforward: those correspond mainly to CH_x deformation modes. In Table 1 an attempt was made to further differentiate between methyl and methylene groups, and also between the methyl moieties directly bonded to the nitrogen atoms and those within the ethyl moieties. Below 1350 cm^{-1}, most peaks are associated with either low-frequency alkyl motions (rockings, waggings, twistings) or C−C or C−N stretchings, and are more mixed.

An assignment that deserves particular attention here is that of the intense peak seen at 975−978 cm^{-1} in the liquid and at 1001−1008 cm^{-1} in the gas. That mode has been traditionally associated with a NC_2 symmetric stretching,[28,32,63,64] apparently following an early assignment made by Bürger et al.[56] However, a couple of reasons made us reassign it to a methyl rocking instead: (1) this mode is in a frequency range typical of methyl rocking motions, as reported for many other compounds,[65] and (2) the position of this peak is highly influenced by the phase in which the compound is in, shifting by ∼30 cm^{-1} between the gas and liquid phases. We assign the NC_2 asymmetric stretching, which is mostly associated with the carbon−ethyl bond, to the peak at ∼1050 cm^{-1} (in the liquid) instead, as suggested by some calculations.[51] The proper identification of these vibrational modes may in principle be quite important here, because they have been used to follow the decomposition of some tetrakisamido metal precursors,[30,36,58,60,62] but in fact the issue is not as crucial because both of the peaks in discussion typically display similar intensity changes upon thermal treatment of the metal amido compounds. In any case, these methyl rocking and C−N stretching modes are likely to be highly mixed.[49,50] Assignment of the 948 cm^{-1} peak in TDMAT to a Ti−N stretching[58] is less justifiable.

As already mentioned, the IR region above 1600 cm^{-1} is basically flat for all three TEMAM studied here. This is what is expected, since peaks in this region would imply the existence of multiple bonds and none are present in the original amido compounds. It should be pointed out, however, that a small feature is observed around ∼1640 cm^{-1} in some of the spectra obtained in the gas phase. This signal is likely to originate from a decomposition product and could correspond to the stretching of one or more carbon−nitrogen double bonds, but since it is also accompanied by an additional broad band around 3250 cm^{-1}, it may more likely be associated with an amine: the values of 1640 and 2350 cm^{-1} are typical of N−H deformation and stretching modes, respectively. The TEMAM compounds in these experiments were mildly heated in order to vaporize them into the IR cell, and that is known to induce some thermal decomposition. Indeed, TDMAT has been reported to produce dimethylamine in the gas phase at temperatures as low as 375 K.[32,61] Both TDEAT[61] and TDMAZ[60] have proven somewhat more stable, but they also decompose slowly over time. TEMAT has been reported to produce imines and nitriles upon heating above 575 K.[62]

Finally, the third region in the IR spectra in Figure 3, that between 2700 and 3100 cm^{-1}, corresponds to the C−H stretching modes within the amine moieties, and is somewhat tricky to assign. The data in this region can nevertheless be quite informative, especially when following the thermal chemistry of the TEMAM compounds. For the assignment of this region of the spectra, in addition to using the reference compounds listed above, a comparison with the spectra of a series of relevant amines[66] was carried out, as summarized in Figure 4. The final assignment is also provided in Table 1.

3.2. TEMAM Uptake on Silicon Surfaces. The adsorption and reactivity of TEMAM on the surface of an untreated Si(100) wafer, which is covered by a thin film of a naturally formed oxide,[41] was probed next. To estimate the temperature range of interest for our studies, the initial uptake experiment were carried

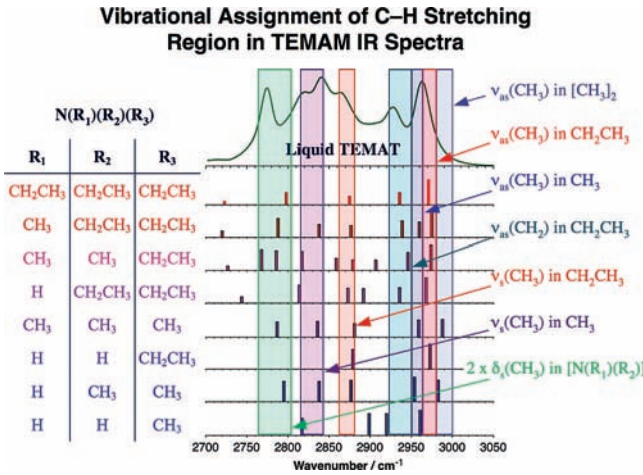

Figure 4. Assignment of vibrational modes for TEMAT in the C−H stretching mode region. A comparison is provided with data from the family of free amines listed on the left, shown as bar graphs with relative intensities extracted from reported spectra.[66] The vibrational modes were identified by grouping regions of the spectra according to the nature of the alkyl moieties in the different amines, and the final assignment listed in Table 1.

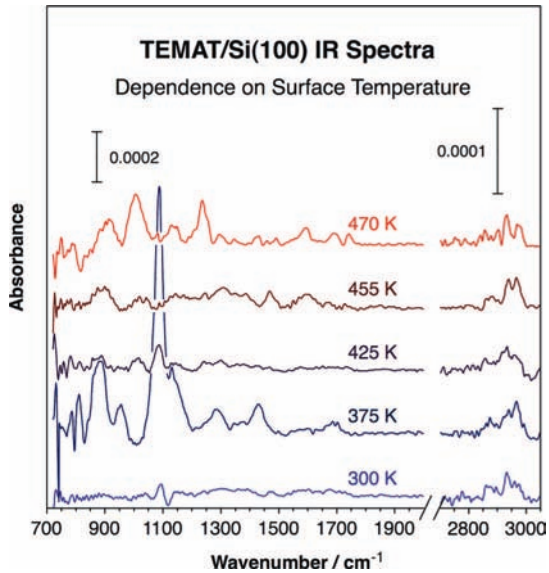

Figure 5. Transmission infrared absorption spectra for TEMAT adsorbed on the surface of a Si(100) wafer as a function of surface temperature. The substrate was untreated, and therefore covered with its native thin film of silicon oxide. Doses of approximately 10 Torr of TEMAT for 10 min were used in all cases.

out with TEMAT at different surface temperatures. Figure 5 reports the transmission infrared absorption spectra obtained after dosing 6×10^9 L (10 Torr for 10 min) of TEMAT at different temperatures between 300 and 470 K. A few preliminary experiments were also carried out with TEMAZ and TEMAH (data not shown): they show similar chemistry, but also highlight the higher stability of those compounds.

The experiments indicated that at room temperature (300 K), the uptake of TEMAT on the surface is minimal. Indeed, virtually no infrared absorption signal is seen in the corresponding trace below 2000 cm^{-1}. A few peaks are seen in the C−H stretching region, but those may be due to contaminants, or perhaps to a signal miscancellation during the ratioing against the background spectrum. At 375 K, by contrast, quite intense features are seen throughout the whole spectral range investigated. The most prominent peak is seen at 1085 cm^{-1}, most likely due to a C−N stretching mode, ν_s(C−N−C), even though that is blue-shifted somewhat from where it is seen in the spectra of the free TEMAT. Additional broad features are also seen at 808, ∼880, 948, 1128, 1283, and 1426 cm^{-1}, modes that can be assigned to a methylene rocking, $\rho(CH_2)$, mixtures of methyl rocking and carbon−carbon stretching, $\rho(CH_3) + \nu$(C−C), (two modes), another nitrogen−carbon stretching, ν_{as}(C−N−C), a methylene wagging, $\omega(CH_2)$, and a methyl asymmetric deformation, $\delta_{as}(CH_3)$, respectively. In the C−H stretching region the dominant peaks are seen at 2872, 2938, and 2967 cm^{-1}, and potentially correspond to $\nu_s(CH_3)$, $\nu_{as}(CH_2)$, and $\nu_{as}(CH_3)$ modes, respectively. The richness of this spectrum and its similarity with that of liquid TEMAT suggest minimum decomposition upon adsorption at this temperature, or at least the survival of some of the ethylmethylamido (EMA) moieties. On the other hand, a few of these peaks undergo measurable shifts, and their relative intensities are fairly different than in the free molecule. It could be argued that adsorption may take place with loss of some of the ethylmethylamine (EMA) ligands, as suggested previously,[63] but the changes in relative intensities also may be related to specific adsorption geometries.[67,68] In any case, it can be said that at this stage the adsorbate is only partially decomposed if at all, and that it still has some EMA ligands attached to the Ti metal center.

Most of the peaks seen at 375 K are gone by 425 K. At that temperature a small feature is still observable at 1082 cm^{-1}, indicating incomplete decomposition and suggesting the survival of small amounts of the EMA ligand, but even that feature disappears by 455 K. The spectra obtained at higher temperatures are somewhat noisy and their reproducibility poor, but they are different enough from those obtained at lower temperatures to confidently indicate that the original amido ligands have been either ejected from the surface or transformed into other species. Importantly, a clear and relatively sharp set of new peaks develops in the C−H region at this stage (see below). The main conclusions at this point are the following: (1) adsorption of TEMAT on the untreated Si(100) wafer appears to occur with the loss of some EMA ligands but also with the preservation of others; (2) further thermal chemistry of the resulting adsorbates starts at temperatures as low as 425 K and leads to the loss of all EMA signatures; and (3) by approximately 475 K another distinct organic moiety forms on the surface. The identity of that moiety was investigated in more detail, and is discussed next.

Typical IR data obtained from Si(100) surfaces exposed to TEMAM at 475 K are displayed in Figure 6. Three traces are shown in that figure, for TEMAT and TEMAZ as obtained with the ATR IR setup, and for TEMAZ as acquired in transmission IR mode. All three traces share the same prominent features, in particular the peaks at approximately 1587, 2855, and 2930 cm^{-1}. A broad, multipeak feature is also seen in two of the three spectra between ∼1400 and 1600 cm^{-1}, possibly due to methyl and methylene deformation modes. The other features proved hard to reproduce, especially those below 1400 cm^{-1}, with the possible exception of the two broad peaks at ∼1000 and 1100 cm^{-1} that likely reflect methyl rocking and C−N stretching motions, respectively. The detection of some molecular vibrational modes speaks to the preservation of at least some of the original ligands on the surface at this temperature. The peak at 1587 cm^{-1}, on the other hand, is characteristic of C═N bonds, and clearly points to partial dehydrogenation of the amido ligands.[32,62] As mentioned in the Introduction, this reaction has been well documented already, appears to take place via a β-hydride elimination step, and most likely leads to the

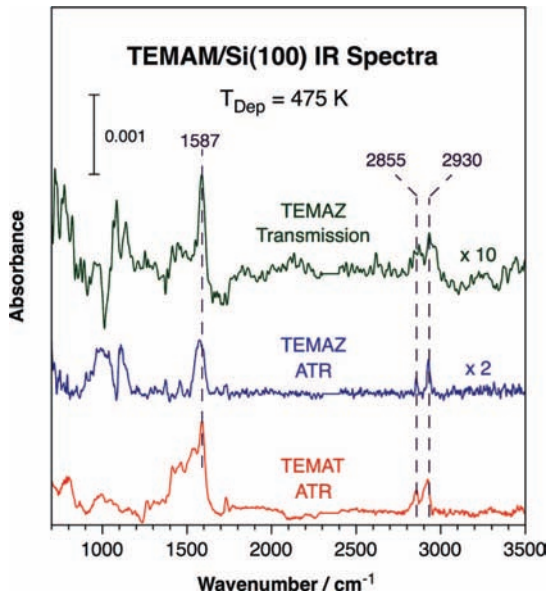

Figure 6. Infrared absorption spectra from Si(100) surfaces after saturation with TEMAM at 475 K. Three traces are shown, for spectra of TEMAT and TEMAZ recorded with use of the ATR IR setup (bottom two traces), and for data of TEMAZ taken with the transmission IR apparatus (top trace). All these spectra share similar prominent peaks at 1587, 2855, and 2930 cm^{-1}, all associated with a surface imine.

formation of an imine ligand.[29,30,36] Such dehydrogenation appears to start at temperatures slightly below 475 K with TEMAT, but only happens after extensive annealing at 475 K with TEMAZ, and is not seen until higher temperatures with TEMAH (data not shown).

A question arises here in terms of the regioselectivity of the β-H dehydrogenation step from TEMAM, because TEMAM contains both methyl and ethyl moieties, so hydrogen abstraction can potentially occur from either hydrocarbon fragment. To address this issue, the spectra of the resulting imine, in particular the peaks seen in the C−H region, were studied in more detail. An assignment of the observed peaks was done by comparison with reported spectra for a number of relevant molecules, including gas- and liquid-phase ethyl cyanade,[69] gas-, liquid-, and solid-phase azidoethane,[70] and gas-phase and Ar-matrix-trapped *N*-methylethylidenimine,[71] as illustrated in Figure 7. It was found that the IR traces for both TEMAT and TEMAZ deposited on Si(100) at 475 K are fairly simple, displaying two main peaks at ∼2855 and 2930 cm^{-1}. The best correspondence is obtained with the spectrum of *N*-methylethylidenimine, with the two peaks most likely corresponding to the symmetric and asymmetric C−H stretching modes of the methyl group directly attached to the nitrogen atom. It has been argued before, based on steric effects, that the β-H elimination step should happen on the methyl moiety instead,[61,62] but this type of reaction is in fact preferred at the inner carbons on other types of adsorbed hydrocarbon moieties,[72−75] and that is consistent with our assignment here. Also to note is the slight shifts in the two C−H stretching bands in the spectra of the species obtained after TEMAM dosing on Si(100) (as compared with the gas-phase imine). This can be explained in terms of a partial rehybridization of the C═N bond to an sp^3 character upon coordination with the Ti or Zr metal.

3.3. TiN Film Growth via Thermal Decomposition of TEMAT. The uptake of TEMAT was also characterized ex situ by XPS. Figure 8 summarizes key data obtained as a function of substrate temperature. Shown are the XPS regions corresponding to Si 2p, N 1s, Ti 2p, and O 1s photoelectrons for samples treated by ten cycles of exposures to 5 mTorr of TEMAT for 1 min (∼300 000 L) each separated by pumping and purging with N_2 while maintaining the surface at 300, 425, and 475 K (bottom three traces). C 1s XPS data were obtained as well. However, because of the incorporation of adventitious carbon on the surface of samples during their transfer from the IR cell to the XPS system, those results were inconclusive. In all three cases the spectra are dominated by the main Si 2p peak at 99.2 eV corresponding to pure silicon, and by smaller Si 2p and O 1s peaks at 103.2 and 532.5 eV, respectively, associated with the SiO_2 layer present in the nonetched Si(100) wafer.[43] Only at 475 K there is evidence for some TEMAT adsorption, as evidenced by the small Ti $2p_{3/2}$ and $2p_{1/2}$ signals at approximately 458.8 and 464.6 eV, respectively. Both the peak positions and the magnitude of the spin splitting seen here are consistent with titanium in a +4 oxidation state.[38,43] There may also be some signal in the N 1s region around 400.0 eV, but it is difficult to establish that with certainty because of the low signal-to-noise ratio of the data. Such a feature would nevertheless be consistent with the presence of imine species on the surface,[76] as determined by IR absorption spectroscopy.

The top trace in Figure 8 was obtained after a continuous 3-h exposure of the Si(100) substrate to 10 mTorr of TEMAT at 475 K, the equivalent of a 10^8 L dose. In this case a thick titanium-containing layer was deposited, thick enough to completely mask the Si 2p signal, and also to generate a copper-like texture, as indicated by simple visual inspection of the surface. The Ti $2p_{3/2}$ peak is centered at 458.8 eV, indicating again the deposition of Ti^{4+}, and a strong N 1s signal is seen at 397.1 eV, as expected from the formation of a metal nitride. Two observations preclude us from concluding that a clean TiN film has been deposited: (1) the titanium signal is consistent with a +4, not +3, oxidation state; and (2) strong O 1s XPS signals are seen at 530.8 and 533.2 eV. There appears to be a significant amount of TiO_2 on the surface, perhaps formed during transport of the sample from the reactor to the XPS apparatus. Also, large amounts of carbon are detected by XPS, although, as mentioned above, that could originate from contamination of the sample during transport. Carbon deposition may be expected via thermal decomposition of the imine intermediate identified in this work. On the other hand, additional infrared experiments in our laboratory indicate that the imine can be cleanly displaced by other gases, ammonia in particular (data not shown). More studies are required to better determine the source of the contaminants.

4. Discussion

The infrared absorption spectroscopy and XPS studies reported here were aimed to provide some insights into the chemistry of TEMAM on the surface of Si(100) wafers. Most of the work discussed above was carried out with TEMAT, the most reactive of the three precursors tried, but at least some of the chemistry is expected to be similar with that of the other compounds. Certainly, some mechanistic conclusions can be reached from our results. For one, according to the data in Figure 5, TEMAT can be adsorbed on Si(100) at low temperatures, around 375 K, but that adsorption appears be molecular, or at least reversible; no molecular species remain on the surface after heating to 425 K. Activated and irreversible adsorption is only seen starting around 470 K. A similar conclusion was reached by the ex situ characterization of the samples with XPS, as shown in Figure 8.

By 475 K, both IR and XPS studies show that some TEMAT adsorbs on the surface irreversibly, and also that it undergoes a

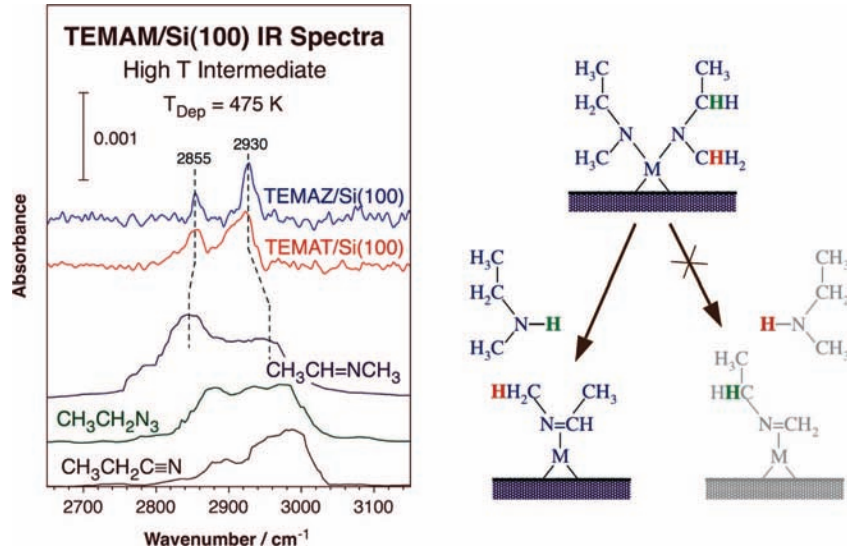

Figure 7. Left: High-frequency region of the infrared absorption spectra of TEMAZ (top trace) and TEMAT (second from top) adsorbed on Si(100) at 475 K. Reference spectra are provided for gas-phase ethyl cyanade (bottom trace),[69] liquid azidoethane (second from bottom),[70] and gas-phase *N*-methylethylidenimine (third from bottom)[71] to aid in the assignment. The data indicate the occurrence of a β-hydride elimination at the ethyl moiety of the ethylmethylamido ligand, as illustrated in the reaction scheme shown on the right.

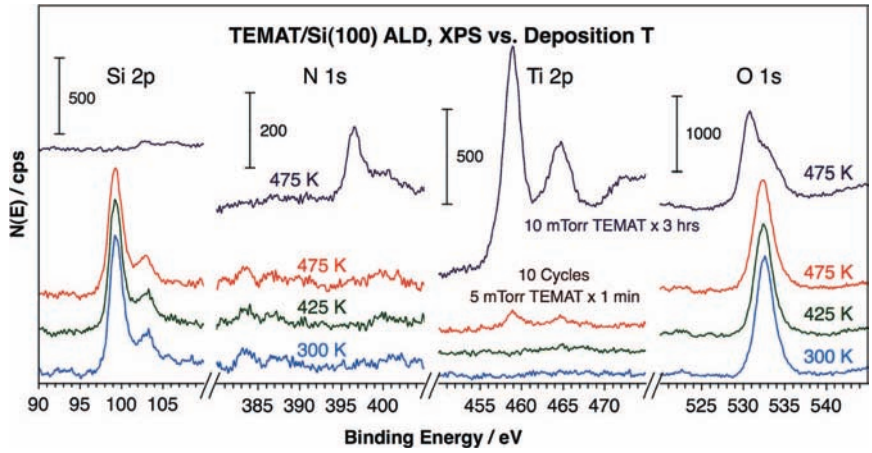

Figure 8. X-ray photoelectron spectra (XPS) of Si(100) surfaces after dosing TEMAT under different conditions. Shown are the Si 2p (far left), N 1s (second from left), Ti 2p (second from right), and O 1s (far right) regions of the spectra for samples obtained after 10 exposures of the surface to 5 mTorr of TEMAT for 1 min at 300, 425, and 475 K (bottom three traces). The sample was always flushed with N_2 in between exposures, as described in the other experiments. Also shown are the data obtained after a continuous flow of TEMAT (at 10 mTorr) for 3 h while keeping the surface at 475 K. The strong peaks seen for Ti and N in the latter sample point to film growth via direct decomposition of the TEMAT precursor.

degree of dehydrogenation in the amido ligands to form an imine intermediate. The imine was clearly identified by the changes in the C−H stretching region of the IR spectra and by the growth of a new peak at 1587 cm^{-1} due to a C═N stretching vibration mode (Figure 6). The β-hydride elimination that leads to the formation of this intermediate has in fact been reported before for other metal amido complexes,[29,30,36] and also for TEMAT in the gas phase.[62] What is new here is the fact that, since the amido ligands in the TEMAM precursors contain two different alkyl moieties (one methyl and one ethyl), two different β-hydride elimination steps are possible. The assignment of the C−H stretching modes of the imine reported in Figure 7 led to the determination that the dehydrogenation occurs preferentially at the ethyl moiety and that such reaction results in the formation of a *N*-methylethylidenimine surface species. This is a surprising result, because in the past it has been shown that diethylamido metal complexes are more stable and decompose at higher temperatures than equivalent dimethylamido compounds.[61] On the basis of that, it would have been reasonable to predict the β-H elimination to occur selectively at the methyl moiety, not at the ethyl end as seen here. On the other hand, the β-hydride elimination from the more substituted carbon, as seen here, is in line with chemistry typical of alkyl moieties adsorbed on surfaces.[72−75] In any case, the implication from the β-hydride elimination at the ethyl position is that that step must take place rapidly following another preceding rate-limiting step during the dissociative adsorption of the metal amido compounds. That step is likely to involve the elimination of some of the initial amido ligands in the TEMAM complex.

5. Conclusions

Infrared absorption and X-ray photoelectron spectroscopy results from a study of the surface chemistry of tetrakis(ethylmethylamido)metal (TEMAM) complexes in relation to their role in atomic layer deposition (ALD) processes were reported. A number of conclusions regarding the mechanism of adsorption and reactivity of TEMAM complexes with titanium, zirconium,

and hafnium on (100)-oriented silicon wafers were reached, some new and some consistent with previous work:

(1) Initial adsorption is dissociative at the temperatures typically used for ALD, and no significant reactivity or uptake is seen below approximately 450 K.

(2) At temperatures of about 475 K adsorption does occur, but it is accompanied by the formation of imine moieties.

(3) The new imine species are produced via β-hydride elimination from some of the original amido ligands.

(4) The β-hydride elimination step occurs preferentially on the ethyl moiety of the ethylmethylamido ligands, and leads to the production of *N*-methylethylidenimine.

(5) Given the known lesser reactivity of metal precursors with diethylamido compared to dimethylamido ligands, the preference for β-hydride elimination from the ethyl end of methylethylamido ligands suggests that this is not the rate-limiting step in the adsorption. The elimination of some of the original amido ligands probably is.

(6) Long exposures of the surface to TEMAT at temperatures above 475 K lead to the growth of thick titanium nitride films. These films do contain significant amounts of C and O contaminants, and are also easily oxidized upon exposure to air.

(7) CVD growth is difficult to avoid. This is because relatively high temperatures are required to promote the activated adsorption of the TEMAM, and that triggers further decomposition of the ligands.

Acknowledgment. Funding for this project was provided by a grant from the U.S. National Science Foundation.

References and Notes

(1) Elam, J. W.; Schuisky, M.; Ferguson, J. D.; George, S. M. *Thin Solid Films* **2003**, *436*, 145.
(2) Becker, J. S.; Kim, E.; Gordon, R. G. *Chem. Mater.* **2004**, *16*, 3497.
(3) Schaeffer, J.; Edwards, N. V.; Liu, R.; Roan, D.; Hradsky, B.; Gregory, R.; Kulik, J.; Duda, E.; Contreras, L.; Christiansen, J.; Zollner, S.; Tobin, P.; Nguyen, B. Y.; Nieh, R.; Ramon, M.; Rao, R.; Hegde, R.; Rai, R.; Baker, J.; Voight, S. *J. Electrochem. Soc.* **2003**, *150*, F67.
(4) Jones, A. C.; Aspinall, H. C.; Chalker, P. R.; Potter, R. J.; Kukli, K.; Rahtu, A.; Ritala, M.; Leskela, M. *J. Mater. Chem.* **2004**, *14*, 3101.
(5) Choy, K. L. *Prog. Mater. Sci.* **2003**, *48*, 57.
(6) Crowell, J. E. *J. Vac. Sci. Technol. A* **2003**, *21*, S88.
(7) Jones, A. C.; Aspinall, H. C.; Chalker, P. R.; Potter, R. J.; Manning, T. D.; Loo, Y. F.; O'Kane, R.; Gaskell, J. M.; Smith, L. M. *Chem. Vap. Deposition* **2006**, *12*, 83.
(8) Hausmann, D. M.; Kim, E.; Becker, J.; Gordon, R. G. *Chem. Mater.* **2002**, *14*, 4350.
(9) Kim, H. *J. Vac. Sci. Technol. B* **2003**, *21*, 2231.
(10) Ritala, M. Atomic layer deposition. In *High-k Gate Dielectrics*; Houssa, M., Ed.; Institute of Physics: Philadelphia, PA, 2004; pp 17−64.
(11) Xu, Y.; Musgrave, C. B. *Surf. Sci.* **2005**, *591*, L280.
(12) Kukli, K.; Ritala, M.; Sajavaara, T.; Keinonen, J.; Leskelä, M. *Chem. Vap. Deposition* **2002**, *8*, 199.
(13) Hino, S.; Nakayama, M.; Takahashi, K.; Funakubo, H.; Tokumitsu, E. *Jpn. J. Appl. Phys.* **2003**, *42*, 6015.
(14) Liu, X.; Ramanathan, S.; Longdergan, A.; Srivastava, A.; Lee, E.; Seidel, T. E.; Barton, J. T.; Pang, D.; Gordon, R. G. *J. Electrochem. Soc.* **2005**, *152*, G213.
(15) Prybyla, J. A.; Chiang, C. M.; Dubois, L. H. *J. Electrochem. Soc.* **1993**, *140*, 2695.
(16) Fix, R.; Gordon, R. G.; Hoffman, D. M. *Chem. Mater.* **1991**, *3*, 1138.
(17) Lim, G. T.; Kim, D. H. *Thin Solid Films* **2006**, *498*, 254.
(18) Maeng, W. J.; Kim, H. *Electrochem. Solid State Lett.* **2006**, *9*.
(19) Xie, Q.; Jiang, Y. L.; Detavernier, C.; Deduytsche, D.; Van Meirhaeghe, R. L.; Ru, G. P.; Li, B. Z.; Qu, X. P. *J. Appl. Phys.* **2007**, *102*.
(20) Hackley, J. C.; Demaree, J. D.; Gougousi, T. *J. Vac. Sci. Technol. A* **2008**, *26*, 1235.
(21) Kim, J. Y.; Choi, G. H.; Kim, Y. D.; Kim, Y.; Jeon, H. *Jpn. J. Appl. Phys. 1* **2003**, *42*, 4245.
(22) Ohshita, Y.; Ogura, A.; Ishikawa, M.; Kada, T.; Hoshino, A.; Suzuki, T.; Machida, H.; Soai, K. *Chem. Vap. Deposition* **2006**, *12*, 130.
(23) Katamreddy, R.; Inman, R.; Jursich, G.; Soulet, A.; Takoudis, C. *J. Mater. Res.* **2007**, *22*, 3455.
(24) Shin, H. K.; Shin, H. J.; Lee, J. G.; Kang, S. W.; Ahn, B. T. *Chem. Mater.* **1997**, *9*, 76.
(25) Panda, S.; Kim, J.; Weiller, B. H.; Economou, D. J.; Hoffman, D. M. *Thin Solid Films* **1999**, *357*, 125.
(26) Hackley, J. C.; Gougousi, T.; Demaree, J. D. *J. Appl. Phys.* **2007**, *102*, 034101.
(27) McNeill, D. W.; Bhattacharya, S.; Wadsworth, H.; Ruddell, F. H.; Mitchell, S. J. N.; Armstrong, B. M.; Gamble, H. S. *J. Mater. Sci.: Mater. Electron.* **2008**, *19*, 119.
(28) Dubois, L. H.; Zegarski, B. R.; Girolami, G. S. *J. Electrochem. Soc.* **1992**, *139*, 3603.
(29) Dubois, L. H. *Polyhedron* **1994**, *13*, 1329.
(30) Truong, C. M.; Chen, P. J.; Corneille, J. S.; Oh, W. S.; Goodman, D. W. *J. Phys. Chem.* **1995**, *99*, 8831.
(31) Corneille, J. S.; Chen, P. J.; Truong, C. M.; Oh, W. S.; Goodman, D. W. *J. Vac. Sci. Technol. A* **1995**, *13*, 1116.
(32) Driessen, J. P. A. M.; Schoonman, J.; Jensenc, K. F. *J. Electrochem. Soc.* **2001**, *148*, G178.
(33) Ho, M. T.; Wang, Y.; Brewer, R. T.; Wielunski, L. S.; Chabal, Y. J.; Moumen, N.; Boleslawski, M. *Appl. Phys. Lett.* **2005**, *87*, 1.
(34) Wang, Y.; Ho, M. T.; Goncharova, L. V.; Wielunski, L. S.; Rivillon-Amy, S.; Chabal, Y. J.; Gustafsson, T.; Moumen, N.; Boleslawski, M. *Chem. Mater.* **2007**, *19*, 3127.
(35) Rodríguez-Reyes, J. C. F.; Teplyakov, A. V. *J. Phys. Chem. C* **2008**, *112*, 9695–9705.
(36) Beaudoin, M.; Scott, S. L. *Organometallics* **2001**, *20*, 237.
(37) Fix, R. M.; Gordon, R. G.; Hoffman, D. M. *Chem. Mater.* **1990**, *2*, 235.
(38) Tiznado, H.; Zaera, F. *J. Phys. Chem. B* **2006**, *110*, 13491.
(39) Xu, M.; Tiznado, H.; Kang, B.-C.; Bouman, M.; Lee, I.; Zaera, F. *J. Korean Phys. Soc.* **2007**, *51*, 1063.
(40) Tiznado, H.; Bouman, M.; Kang, B.-C.; Lee, I.; Zaera, F. *J. Mol. Catal. A* **2007**, *281*, 35.
(41) *Fundamental Aspects of Silicon Oxidation*; Chabal, Y. J., Ed.; Springer-Verlag: Berlin, Germany, 2001.
(42) Roth, K. M.; Yasseri, A. A.; Liu, Z. M.; Dabke, R. B.; Malinovskii, V.; Schweikart, K. H.; Yu, L. H.; Tiznado, H.; Zaera, F.; Lindsey, J. S.; Kuhr, W. G.; Bocian, D. F. *J. Am. Chem. Soc.* **2003**, *125*, 505.
(43) *Handbook of X-Ray Photoelectron Spectroscopy*; Wagner, C. D., Riggs, W. M., Davis, L. E., Moulder, J. F., Muilenberg, G. E., Eds.; Perkin-Elmer Corporation: Eden Prairie, MI, 1978.
(44) Durig, J. R.; Cox, F. O. *J. Mol. Struct.* **1982**, *95*, 85.
(45) Batista de Carvalho, L. A. E.; Teixeira-Dias, J. J. C. *J. Raman Spectrosc.* **1995**, *26*, 653.
(46) Durig, J. R.; Zheng, C.; Herrebout, W. A.; van der Veken, B. J. *J. Mol. Struct.* **2002**, *641*, 207–224.
(47) Chen, K.-H.; Lii, J.-H.; Fan, Y.; Allinger, N. L. *J. Comput. Chem.* **2007**, *28*, 2391.
(48) Yoshida, H.; Ehara, A.; Matsuura, H. *Chem. Phys. Lett.* **2000**, *325*, 477–483.
(49) Durig, J. R.; Li, Y. S. *J. Chem. Phys.* **1975**, *63*, 4110.
(50) Hamada, Y.; Hashiguchi, K.; Hirakawa, A. Y.; Tsuboi, M.; Nakata, M.; Tasumi, M.; Kato, S.; Morokuma, K. *J. Mol. Spectrosc.* **1983**, *102*, 123.
(51) Durig, J. R.; Beshir, W. B.; Godbey, S. E.; Hizer, T. J. *J. Raman Spectrosc.* **1989**, *20*, 311.
(52) Buttler, M. J.; McKean, D. C. *Spectrochim. Acta* **1965**, *21*, 465.
(53) Gamer, G.; Wolff, H. *Spectrochim. Acta A* **1973**, *29*, 129.
(54) Murphy, W. F.; Zerbetto, F.; Duncan, J. L.; McKean, D. C. *J. Phys. Chem.* **1993**, *97*, 581.
(55) Durig, J. R.; Lindsay, N. E.; Hizer, T. J.; Odom, J. D. *J. Mol. Struct.* **1988**, *189*, 251.
(56) Bürger, H.; Stammreich, H.; Teixeira Sans, T. *Monatsh. Chem.* **1966**, *97*, 1276.
(57) van der Vis, M. G. M.; Konings, R. J. M.; Oskam, A.; Walter, R. *J. Mol. Struct.* **1994**, *323*, 93.
(58) Yun, J. Y.; Park, M. Y.; Rhee, S. W. *J. Electrochem. Soc.* **1998**, *145*, 2453.
(59) Rodríguez-Reyes, J. C. F.; Teplyakov, A. V. *J. Phys. Chem. C* **2007**, *111*, 4800.
(60) Kim, I.-W.; Kim, S.-J.; Kim, D.-H.; Woo, H.; Park, M.-Y.; Rhee, S.-W. *Korean J. Chem. Eng.* **2004**, *21*, 1256.
(61) Yun, J. Y.; Park, M. Y.; Rhee, S. W. *J. Electrochem. Soc.* **1999**, *146*, 1804.
(62) Kim, S. J.; Kim, B.-H.; Woo, H.-G.; Kim, S.-K.; Kim, D.-H. *Bull. Korean Chem. Soc.* **2006**, *27*, 219.
(63) Maslar, J. E.; Hurst, W. S.; Burgess, D. R., Jr.; Kimes, W. A.; Nguyen, N. V. *ECS Trans.* **2007**, *2*, 133.
(64) Bradley, D. C.; Gitlitz, M. H. *J. Chem. Soc. A* **1969**, 980.
(65) Socrates, G. *Infrared Characteristic Group Frequencies: Tables and Charts*, 2nd ed.; Wiley: Chichester, UK, 1994.

(66) Spectral Database for Organic Compounds, SDBS, National Institute of Advanced Industrial Science and Technology (AIST), Japan, http://riodb01.ibase.aist.go.jp/sdbs/, 2008.
(67) Chabal, Y. J. *Surf. Sci. Rep.* **1988**, *8*, 211.
(68) Zaera, F. *Int. Rev. Phys. Chem.* **2002**, *21*, 433.
(69) Wurrey, C. J.; Bucy, W. E.; Durig, J. R. *J. Phys. Chem.* **1976**, *80*, 1129.
(70) Nielsen, C. J.; Kosa, K.; Priebe, H.; Sjøgren, C. E. *Spectrochim. Acta A* **1988**, *44*, 409.
(71) Hollenstein, H.; Günthard, H. H. *Chem. Phys. Lett.* **1974**, *4*, 368.
(72) Zaera, F. *Chem. Rev.* **1995**, *95*, 2651.
(73) Tjandra, S.; Zaera, F. *J. Am. Chem. Soc.* **1995**, *117*, 9749.
(74) Jenks, C. J.; Bent, B. E.; Zaera, F. *J. Phys. Chem. B* **2000**, *104*, 3017.
(75) Ma, Z.; Zaera, F. *Surf. Sci. Rep.* **2006**, *61*, 229.
(76) Louette, P.; Bodino, F.; Pireaux, J.-J. *Surf. Sci. Spectra* **2005**, *12*, 54.

JP8102172